Biochemistry

 Volume 40, Number 40 October 9, 2001

Articles

Reduced Outer Membrane Permeability of *Escherichia coli* O157:H7: Suggested Role of Modified Outer Membrane Porins and Theoretical Function in Resistance to Antimicrobial Agents†

Michael B. Martinez, Michael Flickinger, LeeAnn Higgins, Thomas Krick, and Gary L. Nelsestuen*

Department of Biochemistry, Molecular Biology, and Biophysics, University of Minnesota, St. Paul, Minnesota 55108

Received May 9, 2001; Revised Manuscript Received July 27, 2001

ABSTRACT: Outer membrane permeability of *Escherichia coli* O157:H7 was determined by an in vivo kinetic model with the periplasmic enzyme alkaline phosphatase [Martinez et al. (1996) *Biochemistry 35*, 1179−1186]. *p*-Nitrophenyl phospate (PNPP) substrate, added to intact bacteria, must diffuse through the outer membrane to reach the enzyme. At low substrate concentration the bacterium was in the perfectly reactive state where all molecules that entered the periplasm were captured and converted to product. Transmembrane diffusion was rate limiting, and the permeability of the outer membrane was determined from kinetic properties. The O157:H7 strain grown at 30 °C showed one-sixth the permeability of wild-type *E. coli* grown at 30 °C. Wild-type bacteria grown at ≥37 °C show a physiological response with a shift in expression of outer membrane porins that lowered permeability to PNPP by approximately 70%. The O157:H7 strain did not display this temperature-sensitive shift in permeability even though a change in porin expression could be visualized by staining intensity of Omp F and Omp C on acrylamide gels. Altered behavior of the O157:H7 membrane was also indicated by a several thousand-fold lower response to transformation relative to wild-type *E. coli*. Matrix-assisted laser desorption ionization time of flight mass spectrometry and electrospray ionization mass spectrometry confirmed the expression of the Omp F and Omp C variants that are unique to *E. coli* O157:H7. This reduced outer membrane permeability can contribute to enhanced resistance of O157:H7 to antimicrobial agents.

Escherichia coli strain O157:H7, an intestinal bacterium present in beef, has been responsible for outbreaks of infection in many parts of the world (*1*, *2*). *E. coli* O157:H7 has phage-derived DNA that codes for a shiga-like toxin (*Shigella dysenteriae*) (*3*, *4*) that interacts with the globotriaosylceramide (Gb_3) receptor on host cell membranes. The active subunit inhibits protein synthesis (*5*−*8*). Initial infection by *E. coli* strain O157:H7 occurs when bacteria enter the body through the stomach. Survival of only a few bacteria is sufficient for intestinal colonization, proliferation, and toxin synthesis (*1*, *9*). Infection can lead to bloody diarrhea and, in children and compromised humans, hemolytic uremic syndrome (*6*, *8*, *10*−*12*). Undercooked feces-contaminated hamburger can contain *E. coli* O157:H7 so that beef irradiation is frequently employed to combat transmission (*13*). However, infectious outbreaks of *E. coli* O157:H7 also arise from contaminated well water (*14*−*16*).

A feature of *E. coli* strain O157:H7 is its ability to survive in hostile microenvironments. A possible contributor to the

† This work was supported by Grant HL60859 from the Heart, Lung, and Blood Institute, National Institutes of Health. M.B.M. was supported by a supplement to this grant for support of a Minority Investigator.

* To whom correspondence should be addressed. Telephone: (612) 624-3622. Fax: (612) 625-5780. E-mail: nelse002@tc.umn.edu.

10.1021/bi0109515 CCC: $20.00
Published on Web 09/15/2001

molecular basis of superior survival may be an altered outer membrane, which creates resistance to acidic stomach pH (*17*−*19*), bile salts, dilute environments such as well water, and other antimicrobial conditions (*1*). Recently, the sequence of the complete genome of *E. coli* O157:H7 has been determined (*20*). The two major outer membrane proteins, Omp F and Omp C, which act as general diffusion pores (*21*), differ from wild-type *E. coli*. The significance of these changes is not known.

E. coli O157:H7 has resistance to sulfisoxazole, streptomycin, and tetracycline (*22*, *23*). Bacteria can achieve additional protection from these and other antimicrobial agents by limiting access to the bacterium. Reduction of outer membrane permeability is one target of change. The effectiveness of antibiotic detoxifying enzymes such as β-lactamase and/or pumps that expel antibiotics [tetracycline (*24*−*26*)] can be augmented by limiting entrance of the antibiotic through the outer membrane. Thus, quantitative analysis of substrate entry into the periplasm and knowledge of concentration in the periplasm can provide insight into bacterial physiology and survival mechanisms.

Previously, an enzyme kinetic model was developed that precisely described the kinetic behavior of periplasmic alkaline phosphatase. The model was used to determine outer membrane permeability of *E. coli* strains that expressed various outer membrane porins (*27*, *28*). This model was expanded to include the kinetic behavior of periplasmic β-lactamase and the effect of an enzyme inhibitor (*28*, *29*). For several metabolites, including substrates of alkaline phosphatase and β-lactamase, it appeared that normal enzyme expression levels in the periplasm were sufficient to reach the perfectly reactive state where all molecules entering the periplasm were converted to product. Equilibrium between internal (periplasmic) and external substrate levels occurred at extremely high external concentrations that are unlikely to occur.

This study applied the alkaline phosphatase kinetic model to *E. coli* strain O157:H7. The outer membrane of this bacterium was shown to be much less permeable than that of wild-type *E. coli*. Furthermore, the permeability to PNPP[1] did not change in response to growth temperature, a normal physiological response that arises from changes in porin expression by wild-type *E. coli* (*27*−*29*). While expression of the dominant porins, Omp F and Omp C, in O157:H7 was verified by mass spectrometry analysis, gel electrophoresis suggested multiple porins that may contain additional modifications. Expansion of an earlier theoretical model illustrated an enormous potential to enhance resistance to antibiotics by altering porin expression levels as well as the properties of the enzyme. The results also suggest methods that might allow screening for reagents which abolish the unique outer membrane properties of O157:H7, a goal that may assist in overcoming altered membrane permeability as a cellular mechanism of antibiotic resistance.

MATERIALS AND METHODS

Plasmid Transformation. The plasmid pIV26 (*30*) and standard methods of transformation were described previously (*27*, *31*). Briefly, *E. coli* cultures (10 mL) were grown in SOC media (20 g of tryptone, 5 g of yeast extract, and 0.5 g/L NaCl, pH 7.5, containing 1% glucose and 20 mM $MgCl_2$), harvested by centrifugation, and resuspended in 60 mM $CaCl_2$ for 20 min. Plasmid concentration was determined by $1A_{260} = 50$ μg/mL (*32*). Plasmid (0.1 μg, $A_{260/280} = 1.9$) was added to competent *E. coli* cells, and the mixture was put an ice for 30 min. The cells were then placed in a water bath at 42 °C for 90 s and then on ice. Media (SOC, 0.5 mL) was added to the cells, and the mixture was incubated at 37 °C for 60 min. The cells were plated on SOC agar plates (15 g of agar/L) containing ampicillin (100 μg/mL) for selection of colonies containing the pIV26 plasmid and on plates without ampicillin to verify the viability of treated cells. The average number of colonies for three plates is reported. Simultaneous transformations were carried out with *E. coli* strains K12 and O157:H7 (*23*) (American Type Culture Collection).

A stringent protocol was used to achieve transformation of *E. coli* O157:H7. The protocol was essentially the same except that the $CaCl_2$-resuspended cells were left on ice overnight. Competent cells were incubated with plasmid (0.25 μg, $A_{260/280} = 1.9$) for 2 h, and then the cells were incubated at 42 °C for 2.5 min. Again, simultaneous transformations were conducted for *E. coli* K12 and O157:H7. In both cases, plates were incubated overnight and colonies were counted. Appropriate controls were conducted to verify the viability of treated cells.

Cell Growth. Colonies of transformed *E. coli* strains were grown overnight in SOC media and stored at −70° C in fresh media containing 100 μg/mL ampicillin and 20% glycerol. Freezer cultures were used to inoculate fresh media for experiments. Overnight cultures were grown in SOC at 30 °C and used to inoculate fresh tryptone media [10 g of bactopeptone, 5 g/L NaCl (*33*)] to obtain cells in logarithmic growth. Cells were kept on ice overnight and used for kinetic experiments the next day.

Enzyme Assays. Cells were harvested by centrifugation for 10 min at 3000*g* and resuspended in MOPS buffer (0.1 M MOPS, pH 7.2, 0.086 M NaCl, and 1 mM $MgCl_2$). Methods for determination of cell number and enzyme concentration per cell were described previously (*27*). The assay of periplasmic alkaline phosphatase was conducted as described previously, with some modifications (*27*, *33*). Briefly, reaction velocity was determined by monitoring PNPP hydrolysis at 405 nm using a Milton Roy Spectronic 601 spectrophotometer. All components of the reaction were kept on ice and added to heated buffer (37 °C) just prior to assay. Readings were taken every 15 s for a total of 2 min. Three of these assays were conducted, and the average with standard deviation (SD) is reported.

Cell growth and assay were conducted in a BL2 facility, approved by the University of Minnesota Biosafety Committee Biological Safety Officer. All solutions and containers which were used for O157:H7 were treated with 5.25% bleach solution or were autoclaved before being discarded.

Porin Identification. Cultures (50 mL) were grown overnight in tryptone media at temperatures known to induce the synthesis of different porins (30−40 °C). Membrane isolation was accomplished by a published protocol (*34*). Briefly, cells were harvested by centrifugation (10 min at 3000*g*) and resuspended in Nanopure water (20 mL). The cells were

[1] Abbreviations: PNPP, *p*-nitrophenyl phosphate; MALDI-TOF, matrix-assisted laser desorption ionization time of flight; ESI, electrospray ionization; MS, mass spectrometry; ppm, parts per million; TFA, trifluoroacetic acid.

disrupted by passage through a French press two times at 15 000 lbs/in.^{2} or until disruption was evident by decreased turbidity. The broken cells were centrifuged (10 min at 3000*g*), and the supernatant was recentrifuged (10 min at 3000*g*) to eliminate cell debris. The supernatant was centrifuged again (20 min at 12000*g*), and the pellet was resuspended in 5 mL of Nanopure water. The pellet was washed two additional times and resuspended in the sample buffer for SDS−polyacrylamide gel electrophoresis (SDS−PAGE) and boiled for 5 min. Electrophoresis was carried out according to Laemmli (*35*) with 12% gel containing 5 M urea (*34*). The gel was stained with silver (Bio-Rad Inc.) according to the manufacturer's protocol.

In-Gel Tryptic Digest. Protein bands from the gel, along with blank areas of the gel to provide background samples, were excised from the gel, and in-gel tryptic digests were conducted by published methods (*36*), with some modification. Briefly, silver-stained bands were destained with a 1:1 solution of potassium ferricyanide (30 mM) and sodium thiosulfate (100 mM) for 8 min and then washed in 1.0 mL of Nanopure water (four times for 8 min each). The gel slices were covered with acetonitrile for 15 min, the solvent was decanted, and the gel slices were dried by speed vacuum. Dried gel slices were covered with a solution of ammonium bicarbonate (50 mM) containing $CaCl_2$ (5 mM) and sequence grade modified porcine trypsin (12 ng/μL, Promega). This mixture was kept on ice for 1 h and then at 37 °C overnight. The supernatants from the overnight incubations were removed and transferred to a different tube. The gel slices were washed once with 20 mM ammonium bicarbonate (20 min) and three times with 50% acetonitrile−5% formic acid. All supernatants were pooled and speed vacuumed to dryness. For ESI mass spectral analysis, SDS−PAGE bands 1−4 were digested as one and resuspended in sample solution (H_2O−acetonitrile, 96:4, containing 0.2% acetic acid) and kept frozen at −70 °C.

Samples were prepared for MALDI-TOF MS with a Millipore $ZipTip_{C18}$, according to the manufacturer's protocol. Briefly, the dried samples were resuspended in 30 μL of sample solution containing 0.1% TFA (trifluroacetic acid). The $ZipTip_{C18}$ was washed twice with a solution of 50% acetonitrile−Nanopure water (v/v) containing 0.1% TFA and twice with sample solution. The resuspended sample was then slowly aspirated in and out of the tip a minimum of 10 times. The tip was then washed 10 times with the sample solution. Peptides were finally eluted by aspirating 4 μL of ice-cold 75% acetonitrile−Nanopure water (v/v) containing 0.1% TFA.

MALDI-TOF Mass Spectral Analysis. A saturated solution of α-cyano-4-hydroxycinnamic acid (Hewlett-Packard) in methanol was diluted 1:1 with 50% acetonitrile−Nanopure water (v/v) containing 0.1% TFA. This was used as the crystal matrix. Sample and matrix (1:1) were applied to the sample target and air-dried. The instrument used for the collection of MALDI-TOF mass spectrometric data was a Bruker Biflex III, equipped with a N2 laser (337 nm, 3 ns pulse length) and a microchannel plate (MCP) detector. The data were collected in the reflectron mode, positive polarity, with an accelerating potential of 19 kV. Each spectrum is the accumulation of 200 laser shots. External calibration was performed using human angiotensin II [monoisotopic mass [MH^+] 1046.5 (Sigma Chemical Co.)] and adenocorticotropin hormone fragment 18−39 [monoisotopic mass [MH^+] 2465.2 (Sigma Chemical Co.)]. For PSD experiments (positive polarity) an acceleration voltage of 19 kV was lowered to 0.67 kV in 16 steps. Theoretical ions were obtained from DNA sequences and the Protein Prospector MS-Product program (University of California−San Fransisco).

Scheme 1

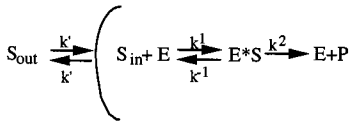

ESI Mass Spectral Analysis. Mass spectra were obtained in positive ion mode with an ion trap mass spectrometer (Thermo Finnigan, LCQ Classic) equipped with a Nano ESI stage (New Objective, Pico View). Peptides were separated on a 75 μm column (Pico Frit Tip, PF360-75-15-N-5, New Objective) packed in-house with C18 packing material (5 μm particle, 200 Å pore diameter, Michrom BioResources Inc.). Peptides were applied to the column, washed with 98:2 H_2O−acetonitrile, containing 0.2% acetic acid, and eluted with a linear gradient (4%/min) of up to 2:98 H_2O−acetonitrile, containing 0.2% acetic acid, by a Magic 2002 HPLC system (Michrom BioResources, Inc). Typically, *X*calibur tripleplay or data-dependent programs in the ms/ms instrument configurations were used with and without exclusion lists and/or parent ions. Peptide search analysis was conducted with Sequest using databases that were modified to contain *E. coli* K12 and O157:H7 Omp F and Omp C amino acid sequences.

3D Model of Omp F. The 3D model of Omp F was obtained through the Swiss model (*37*−*39*) and manipulated to show the desired amino acids by the Rasmol program.

Modeling of Substrate Concentration in the Periplasm. Substrate from the environment enters the periplasm by diffusion through the outer membrane (Scheme 1), a nonsaturable first-order process. Substrate diffusion out of the periplasm is described by the same rate constant.

At steady state, substrate concentration in the periplasm ($[S_{in}]$) is constant and the velocity of diffusion into the periplasm ($k'[S_{out}]$) equals the rate of diffusion out ($k'[S_{in}]$) plus the rate of enzymatic degradation ($v = V_{max}[S_{in}]/(K_M + [S_{in}])$. Combination of these relationships gave eq 1.

$$k'[S_{out}] = k'[S_{in}] + (V_{max}[S_{in}])/(K_M + [S_{in}]) \quad (1)$$

The rate constant for diffusion across the outer membrane can be estimated from the velocity at half of V_{max}. At $V_{max}/2$, $[S_{in}]$ equals the K_M for alkaline phosphatase [15 μM (*28*)]. The velocity of substrate diffusion out of the periplasm ($k'[S_{in}]$) was negligible at 15 μM $[S_{in}]$ so that $k'[S_{out}] = V_{max}/2$. Substitution of $k' = V_{max}/(2[S_{out}]_{0.5})$ into eq 1 produces a quadratic (eq 2, where $W = {}^1/_2[S_{out}]_{0.5}$) which can be solved

$$W[S_{in}]^2 - [S_{in}](WK_M + 1 - W[S_{out}]) + W[S_{out}]K_M \quad (2)$$

over the full substrate ($[S_{out}]$) range. The only experimental parameters needed to model this reaction are K_M for the enzyme and $[S_{out}]_{0.5}$.

RESULTS

Plasmid Transformation. Plasmid transformation requires disruption of cell membranes with calcium chloride or

Table 1: *E. coli* Transformants (Plasmid pIV26) per Microgram of DNA

K12	O157:H7	cells/plate
normal conditions		
3370 ± 120	0	1.84×10^8
360 ± 40	0	1.84×10^7
40 ± 20	0	1.84×10^6
stingent conditions		
lawn	12 ± 8	1.56×10^8
>4000	0	1.56×10^7
228 ± 24	0	1.56×10^6

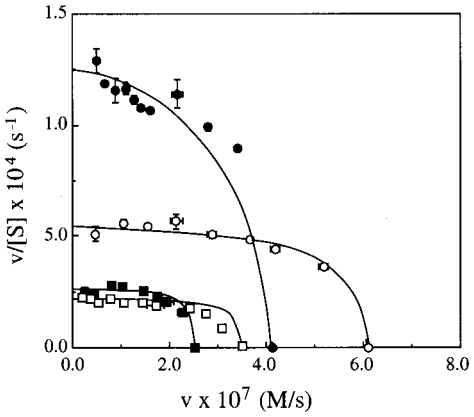

FIGURE 1: Titration of periplasmic alkaline phosphatase. Alkaline phosphatase in the intact bacteria was assayed with PNPP as described for *E. coli* K12 (●, ○) and *E. coli* O157:H7 (■, □) grown at 30 °C (solid symbols) or 40 °C (open symbols). Values and error bars indicate averages and standard deviations of three separate determinations. The solid lines are curves fit to the result by published methods (*28*).

electroporation to allow plasmid entry into the cytoplasm. Rigid membranes might require more stringent methods, and protocols were adjusted to obtain transformants. Two protocols were used (Table 1). The standard protocol provided transformants of *E. coli* K12 but not of O157:H7. In fact, only the highest cell density from the more stringent protocol showed any transformed colonies of O157:H7. Under these conditions, transformed K12 (*E. coli* K12 pIV26) produced a bacterial lawn that could not be counted. Overall, the K12 strain took up plasmid DNA several thousand-fold better than O157:H7. In all cases and with both strains, bacterial lawns were obtained when transformed cells were plated without ampicillin.

Titration of Periplasmic Alkaline Phosphatase. Details of the theory and modeling of enzyme kinetics in the *E. coli* periplasm were presented in an earlier study (*27*, *28*, *40*, *41*). Briefly, access of PNPP to enzyme in the periplasm requires diffusion through the outer membrane, a process regulated by porin channels. Figure 1 shows the kinetics of alkaline phosphatase plotted in the manner of Eadie and Hofstee. For soluble enzymes, this plot is linear with a slope equal to $-1/K_M$. In contrast, the kinetics of periplasmic enzymes showed nonlinear plots [Figure 1 (*28*)]. At low [S], the number of free enzymes in the periplasm was large so that virtually all of the molecules entering were captured and converted to product. The reaction was limited by diffusion of substrate through the outer membrane, a nonsaturable process that results in the observed curve shape. The value of v/[S] in the horizontal region of the plot was directly proportional to outer membrane permeability and cell

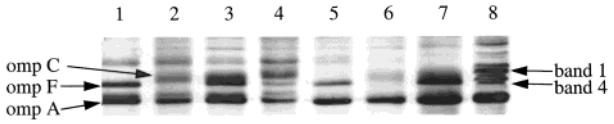

FIGURE 2: Porin expression. Bacterial strains were grown overnight in tryptone broth, and outer membrane proteins were isolated and separated on SDS−PAGE as described. Proteins in lanes 1−4 were isolated from bacteria grown at 40 °C, and those in lanes 5−8 were isolated from bacteria grown at 30 °C. Bacterial strains were as follows: O157:H7 pIV26, lanes 4 and 8; K12 pIV26, lanes 3 and 7; JF703, lanes 2 and 6; and JF701, lanes 1 and 5. Protein band 1 of lane 8 is labeled. Bands referred to as 2, 3, and 4 proceed downward in the gel.

concentration but independent of enzyme concentration in the periplasm (*28*). For easy comparison, the same cell concentrations were used for all titrations in Figure 1.

At high substrate, the number of free enzymes (those with unoccupied substrate binding sites) declined, and efficient capture of substrates entering the periplasm was lost. This produced curvature of the Eadie−Hofstee plot (Figure 1) to a final intercept on the horizontal axis, equal to the traditional V_{max} of the enzyme. The small difference in this value signified a difference in the total number of enzymes per bacterium. This difference does not influence the velocity at low substrate concentration, where enzyme is present in excess (*28*).

At high temperature or osmolarity (Figure 1), previous studies have shown that the dominant porin that is expressed is the more restrictive Omp C. At low temperature or osmolarity, the dominant porin is the less restrictive Omp F (*42*, *43*). In agreement with this response, the lower v/[S] value in the horizontal region of the graph shows that *E. coli* K12 grown at 40 °C had lower outer membrane permeability than when grown at 30 °C (Figure 1). Several determinations gave a 2.5−3.0-fold difference.

E. coli O157:H7 pIV26 showed greatly modified behavior. This strain had lower outer membrane permeability under all growth conditions. In addition, it did not show significant change in membrane permeability due to growth temperature. These unique properties may contribute to the antimicrobial resistance of O157:H7.

Porin Identification. Acrylamide gels of porins from *E. coli* mutants that express Omp C [strain JF703 Δ*ompF* (*44*), Figure 2, lanes 2 and 6] or Omp F [strain JF701 Δ*ompC* (*45*), Figure 2, lanes 1 and 5] are shown in Figure 2 for reference. As expected from published findings (*42*, *43*), wild-type bacteria expressed both porins in a relative abundance that changed with growth temperature. Cells grown at 40 °C (Figure 2, lane 3) gave a higher ratio of Omp C to Omp F than cells grown at 30 °C (Figure 2, lane 7). All strains expressed high levels of Omp A (*21*, *46*), an abundant outer membrane protein (Figure 2). The identity of all bands was confirmed by mass spectrometry, described below.

E. coli O157:H7 (Figure 2, lanes 4 and 8) showed a significantly different set of proteins. When it was grown at 40 °C (Figure 2, lane 4), the migration of the protein bands was similar to wild-type porins, and the dominant protein appeared to be Omp C and a slight shift in Omp C migration could arise from known mutations that give a small molecular weight difference between K12 and 0157:H7. However, when it was grown at 30 °C, a family of bands were pro-

duced that had little resemblance to wild-type porins (Figure 2, lane 8).

MALDI-TOF Mass Spectrometry of Porin Proteins. Mass spectrometry was used to identify the porins in wild-type *E. coli* and to detect other proteins that migrate in this region of the gel. Omp F and Omp C were identified in the correct protein-staining bands from JF703 and JF701 cells (see Figure 2). The *E. coli* genomic data bank provided excellent identification of these proteins. Searches were also conducted for the ions remaining after subtraction of background ions and those from Omp F and C. Very few ions remained, and these did not correlate with known proteins. Thus, it appeared that only Omp F and Omp C were found in this region of the gel.

Four protein-staining bands from *E. coli* O157:H7 (Figure 2, lane 8) were examined. Figure 3A shows the MALDI-TOF spectrum for band 3, identified as Omp F. Figure 3B shows the ions from band 2, identified as Omp C. Although ions from both porins were present in each gel slice, relative levels allowed unambiguous identification. The intensities of parent ions from Omp C were greatest in bands 1 and 2, with a large decrease in transition to band 3 (Table 2). The opposite trend occurred for ions of Omp F, which were most abundant in bands 3 and 4 and showed a large decline in transition to band 2 (Table 2). Background ions were relatively constant. The ion at *m*/*z* of 842.5 arose from trypsin and was present in all samples. The ions identified in Figure 3A corresponded to 71% (10 of 14) of Omp F peptides in the molecular weight range of 450−2000. The peptides labeled in Figure 3B constituted 83% (15 of 18) of the Omp C peptides in the molecular weight range of 450−2000.

Post source decay (PSD) of a peptide from band 2 (Figure 3C, $m/z = 1349.4$) gave 39 ions, 29 (75%) of which matched with ions expected for fragmentation of the corresponding Omp C peptide. PSD of the ion at $m/z = 1849.0$ in Figure 3B gave 36 ions (data not shown), 26 (72%) of which matched expected fragmentation ions for the corresponding Omp F peptide.

Matrix Science Mascot Search (*47*) identified band 2 (Figure 3B) as Omp C with a probability score of 114 and band 3 (Figure 3A) as Omp F with a probability score of 81. These, and similar results obtained for bands 1 and 4, suggested that Omp C was the major protein in bands 1 and 2 while Omp F was the major protein in bands 3 and 4. In all lanes, Omp A was identified by similar methods.

Data searches were conducted with unidentified ions. As for porins of wild-type *E. coli*, subtraction of Omp F, Omp C, and background ions left very few unidentified ions. Data bank searches with those ions did not identify other proteins. Consequently, bands 1−4 of Figure 2, lane 9, appeared to contain only Omp F and Omp C.

Identification of O157:H7 Porins. Omp F of *E. coli* O157:H7 differs from wild-type Omp F by two amino acids (*20*), giving two altered peptides shown by Blast 2 Sequences [Table 3 (*48*)]. Omp C of O157:H7 contains several amino acid substitutions (*20*) from wild-type giving 8 altered peptides shown by Blast 2 Sequences [Table 3 (*48*)]. To ensure that the porins in lane 8 of Figure 2 were those of O157:H7, these peptides were identified by MALDI-TOF and electrospray mass spectrometry. Both of the Omp F peptides unique to O157:H7 were identified by MALDI-TOF (Table 3). Furthermore, the corresponding peptides from wild-type *E. coli* were not detected in these gel slices. Six of the 8 unique peptides of O157:H7 Omp C were identified by MALDI-TOF, while none of the corresponding peptides of wild-type Omp C were found.

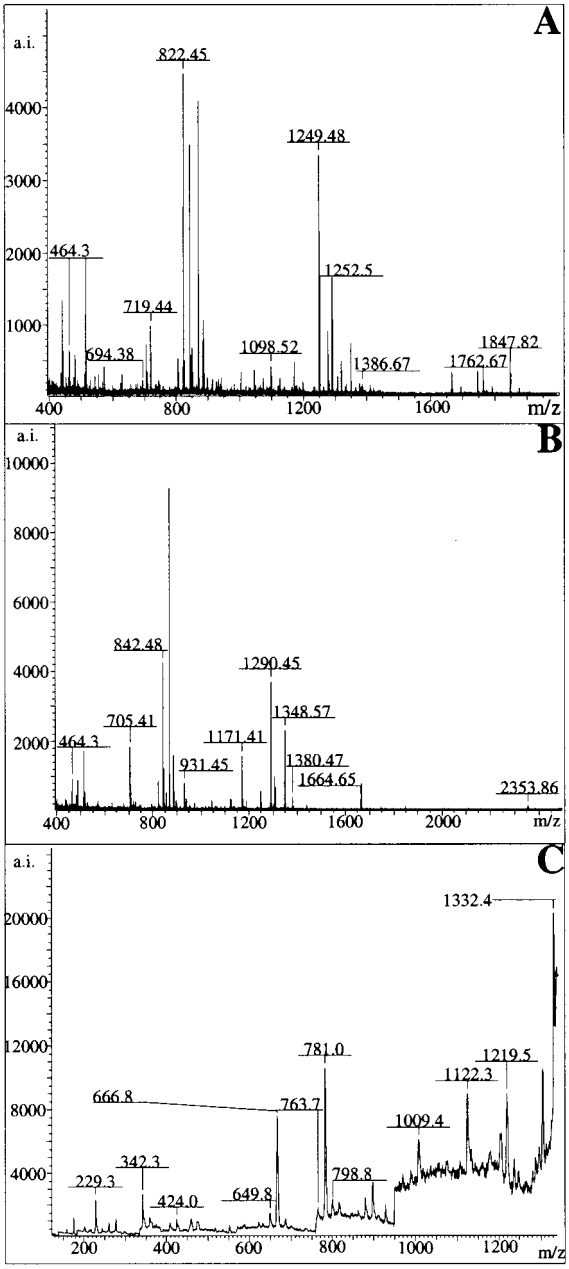

FIGURE 3: Protein identification by MALDI-TOF mass spectrometry. Peptides were released by in-gel digestion of protein bands of *E. coli* O157:H7 and mass spectrometry conducted as described. Panel A: Peptides of band 3 (Figure 2), Omp F. The labeled ions correspond to 10 of the 14 Omp F peptides expected in the molecular weight range of 450−2000. Panel B: Ions of band 2 (Figure 2), Omp C. The labeled ions constitute 15 of 18 Omp C peptides expected in the molecular weight range of 450−2000. Panel C: Post source decay of Omp C ion 1349.4. The labeled ions represent a portion of the 29 ions that corresponded to theoretical breakdown products of the parent peptide. A total of 39 ions were observed.

In-gel digestion of combined bands 1−4 followed by ESI-MS/MS analysis also verified the presence of the O157:H7 peptides (Table 3). Figure 4A shows the base ion trace for porin peptides eluted from a C18 column. A typical MS/MS scan gave signal sufficient for peptide identification and

Table 2: Porin Identification by Ion Intensity[a]

parent ions	SDS−PAGE band						
Omp C		**1348.6**	**1290.6**	**1171.4**	**1124.5**	**939.4**	**885.4**
	1	2.9	4.8	1.8	0.30	0.45	1.5
	2	2.3	3.7	1.6	0.34	0.36	1.5
	3	0.74	1.7	0.48	<0.10	<0.2	0.83
	4	0.32	1.3	0.48	0.13	<0.12	0.62
Omp F		**1249.5**	**1847.8**	**1098.5**	**822.5**	**1386.7**	**1003.5**
	1						
	2	0.55	0.11	0.13	0.87		0.13
	3	3.3	0.41	0.42	4.5	0.18	0.34
	4	2.1	0.23	0.34	2.4	0.14	0.31
background		**515.5**	**1045.8**	**842.5**			
	1	1.1	0.24	3.6			
	2	1.7	0.31	4.2			
	3	1.9	0.37	3.5			
	4	1.5	0.51	3.3			

[a] *m/z* values shown in boldface.

correlation scores by Sequest search. A single run yielded MS/MS of peptides from both Omp F and Omp C. Scan 1025 (Figure 4B) had a parent ion mass of 1386.54 and gave peaks for 20 of 24 b and y ions expected from the corresponding unique peptide 1 of O157:H7 Omp F (Table 3). This gave an excellent correlation score of 4.56. Scan 958 (Figure 4C) of the same run had a parent ion mass of 1665.71 and gave fragmentation ions corresponding to 18 of 28 b and y ions for unique peptide 4 of *E. coli* O157:H7 Omp C (Table 3). The correlation score for this peptide was 3.14. Thus, MALDI-TOF MS and ESI-MS/MS analyses both showed the presence of Omp C and Omp F of *E. coli* O157:H7 in this region of the gel and failed to detect any contaminants.

While the proteins of O157:H7 were clearly identified, the appearance of four or more bands was not explained. It appeared possible that an unidentified modification such as proteolysis or posttranslational modification may occur.

Model of Omp F. While Omp C of O157:H7 has many differences from wild-type protein and changes in its properties may occur, most permeability to PNPP by *E. coli* arises from Omp F (*28*). With only two amino acid differences, the observed large change in permeability was surprising. The substitutions, P226L and T269I, are adjacent in the structure and located near the opening of the Omp F channel (Figure 5, space-filled residues). These changes would not alter surface charge but might cause a decrease in pore size due to altered conformation. Further studies are needed to determine if this is the sole basis for altered permeability.

Theoretical Impact of Altered Permeability on Substrate/Antibiotic Levels in the Periplasm. Documentation of altered membrane permeability of a pathogenic bacterium offered

Table 3: Unique Peptides of O157:H7

Omp F[a]

```
181 GKNERDTARRSNGDGVGGSISYEYEGFGIVGAYGAADRTNLQEAQPLGNGKKAEQWATGL 240
    GKNERDTARRSNGDGVGGSISYEYEGFGIVGAYGAADRTNLQEAQ LGNGKKAEQWATGL
181 GKNERDTARRSNGDGVGGSISYEYEGFGIVGAYGAADRTNLQEAQLLGNGKKAEQWATGL 240

241 KYDANNIYLAANYGETRNATPITNKFTNTSGFANKTQDVLLVAQYQFDFGLRPSIAYTKS 300
    KYDANNIYLAANYGETRNATPITNKFTN SGFANKTQDVLLVAQYQFDFGLRPSIAYTKS
241 KYDANNIYLAANYGETRNATPITNKFTNISGFANKTQDVLLVAQYQFDFGLRPSIAYTKS 300
```

Omp C[a]

```
    MKVKVLSLLVPALLVAGAANAAEVYNKDGNKLDLYGKVDGLHYFSDNKDVDGDQTYMRLG 60
    MKVKVLSLLVPALLVAGAANAAEVYNKDGNKLDLYGKVDGLHYFSD+K VDGDQTYMRLG
    MKVKVLSLLVPALLVAGAANAAEVYNKDGNKLDLYGKVDGLHYFSDDKSVDGDQTYMRLG 60
                                                  c)

121 VTSWTDVLPEFGGDTYGSDNFMQQRGNGFATYRNTDFFGLVDGLNFAVQYQGKNGNPSGE 180
    VTSWTDVLPEFGGDTYGSDNFMQQRGNGFATYRNTDFFGLVDGLNFAVQYQGKNG+ SGE
121 VTSWTDVLPEFGGDTYGSDNFMQQRGNGFATYRNTDFFGLVDGLNFAVQYQGKNGSVSGE 180

181 GFTSGVTNNGRDALRQNGDGVGGSITYDYEGFGIGGAISSSKRTDAQNTAAYIGNGDRAE 240
    G+TNNGR+ALRQNGDGVGGSITYDYEGFGIG A+SSSKRTD QN+  YIGNGDRAE
181 ----GMTNNGREALRQNGDGVGGSITYDYEGFGIGAAVSSSKRTDDQNSPLYIGNGDRAE 236
                                                  c)

301 SKGKNL----GRGYDDEDILKYVDVGATYYFNKNMSTYVDYKINLLDDNQFTRDAGINTD 356
    SKGKNL    GR YDDEDILKYVDVGATYYFNKNMSTYVDYKINLLDDNQFTRDAGINTD
297 SKGKNLGVINGRNYDDEDILKYVDVGATYYFNKNMSTYVDYKINLLDDNQFTRDAGINTD 356
```

OMP	Sequence[b]	[MH+][d]	MALDI-TOF	ESI-MS
F	TNLQEAQLLGNGK	1385.7	X(699)	X
F	FTNISGFANK	1098.6	X(54)	X
C	SVDGDQTYMR	1171.5	X(85)	X
C	NGSVSGEGMTNNGR	1379.6	X(652)	X
C	EALR	488.3	X(41)	X
C	TDDQNSPLYIGNGDR	1664.8	X(30)	X
C	NLGVINGR	842.5	X(24)	X
C	NYDDEDILK	1124.5	X(98)	X
C	FSDDKSVDGDQTY	1329.5		X
C	EGFGIGAAVSSSKRTDDQNSPLY	2399.1		X

[a] The Blast 2 Sequences program was used to align amino acid sequences for wild-type Omp F and Omp C (upper line) with the corresponding porins from O157:H7 (bottom line). Residues in bold show modified peptides. [b] Peptides unique to O157:H7. X indicates identification of the peptide. Error from theoretical mass in parentheses in ppm. [c] Peptides unique to O157:H7 generated by chymotrypsin digestion. [d] Theoretical mass.

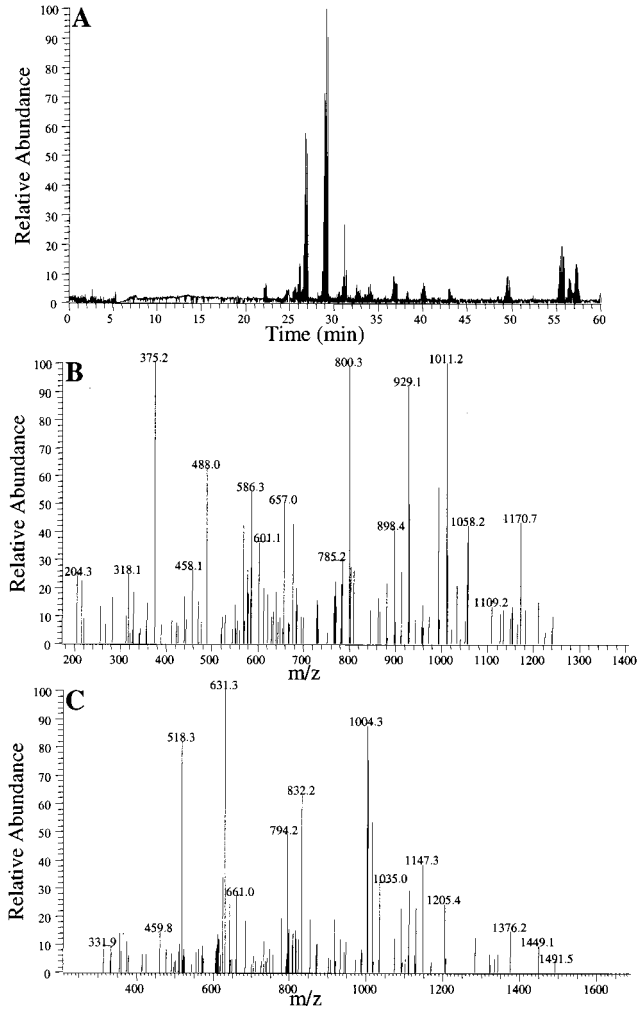

FIGURE 4: Unique peptides of O157:H7. Peptides were released by in-gel digestion of bands 1−4 (Figure 2). Capillary HPLC chromatography and ESI-MS/MS were conducted as described. Panel A: Base peak trace. The intensity of the base peak is shown. Panel B: MS/MS of the 1386.54 parent ion (from panel A). The *m/z* values labeled correspond to 20 of 24 b and y ions from this peptide. Sequest search gave a correlation score of 4.56 to this Omp F peptide. Panel C: MS/MS of the 1665.71 parent ion. The labeled ions correspond to 18 of 28 b or y ions from this Omp C peptide. The Sequest search gave a correlation score of 3.14.

the opportunity to consider theoretical implications for resistance to antimicrobial agents. An altered outer membrane permeability will enhance the resistance to antibacterial agents as a survival mechanism. Even slow diffusion across the outer membrane will eventually produce identical concentrations of agent inside and outside the periplasm. Antimicrobial action can be neutralized by altering enzyme activity or dilution during cell growth.

Theoretical calculations are presented for two systems. The first is alkaline phosphatase, the reaction used in this study. The second is β-lactamase, an enzyme which creates resistance to the penicillin family of antibiotics. Upon entering the periplasm, an antibiotic such as a β-lactam becomes the substrate of two enzymes. The first is the target enzyme, required for cross-linking of peptidoglycan (*49*−*51*). At some level of β-lactam, the activity of this enzyme becomes insufficient to maintain the integrity of the outer membrane. The competing enzyme is β-lactamase, which neutralizes antibiotics. Resistance to β-lactam arises from

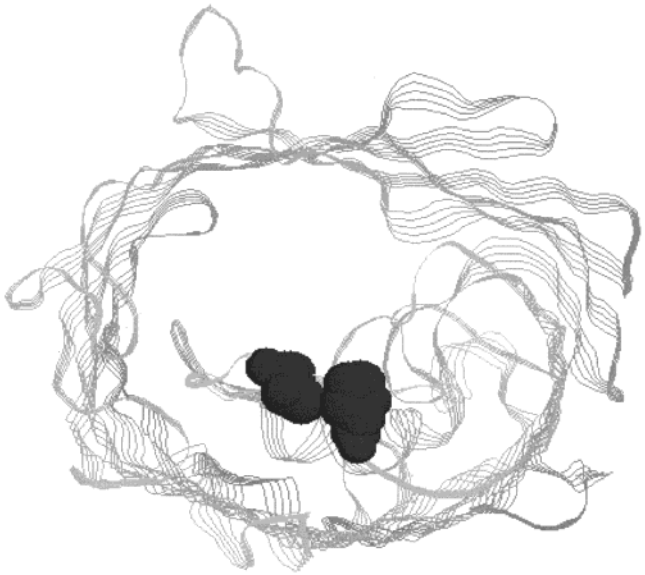

FIGURE 5: Structure of Omp F. The 3D model of Omp F was obtained through Swiss model (*37*−*39*) and is based on the known structure for Omp F (*53*−*55*) and manipulated to show the location of amino acids that are unique to O157:H7. The peptide backbone is shown in ribbon display (Rasmol program) and residues 226 and 269 in space-filled models.

the expression level of β-lactamase, which can maintain the periplasmic concentration of β-lactam at sublethal levels.

The most important parameter is the concentration of substrate inside the periplasm ($[S_{in}]$) as a function of substrate in the environment ($[S_{out}]$). With no enzyme, $[S_{in}]$ increases in parallel with $[S_{out}]$ (Figure 6A). The plots for bacteria containing alkaline phosphatase were obtained from eq 2, using experimentally determined values for K_M (15 μM) and $[S_{out}]_{0.5}$ for bacteria grown at 30 °C (2.37 mM for wild type and 14.5 mM for O157:H7). In this case, $[S_{in}]$ was maintained at low levels, until the enzyme was saturated. Thereafter, $[S_{in}]$ increased in parallel with $[S_{out}]$. Figure 6B shows an expanded scale that emphasizes $[S_{in}]$ at low levels of $[S_{out}]$. Enzymes with a low K_M, such as alkaline phosphatase, maintain very low concentrations of $[S_{in}]$. The reduced outer membrane permeability of O157:H7 extended that region to higher $[S_{out}]$. This shift illustrated the impact of outer membrane permeability on exposure to an external antimicrobial agent.

Also shown are theoretical curves for the enzyme, β-lactamase, and its substrate, cephaloridine. The experimental values for K_M [1.0 mM (*29*)] and $[S_{out}]_{0.5}$ [4.5 mM (*29*)] were used. Comparison to alkaline phosphatase showed the impact of K_M. Due to a high K_M, β-lactamase was less effective in maintaining low $[S_{in}]$. Figure 6B (inset) shows the $[S_{in}]$ for cephaloridine at substrate concentrations that mimic therapeutic levels. For example, the ampicillin concentration used to select tranformants (100 μg/mL) was 0.3 mM. At these concentrations, $[\text{cephaloridine}_{in}]$ was about 0.1 times $[\text{cephaloridine}_{out}]$.

Comparison of results for alkaline phosphatase with those of β-lactamase served to illustrate the potential for evolution of antibiotic resistance. A lowered K_M for β-lactamase would decrease the β-lactam concentration in the periplasm. Reduction of outer membrane permeability would extend the concentration range over which $[S_{in}]$ is reduced. Finally, increase of enzyme concentration will have the same impact

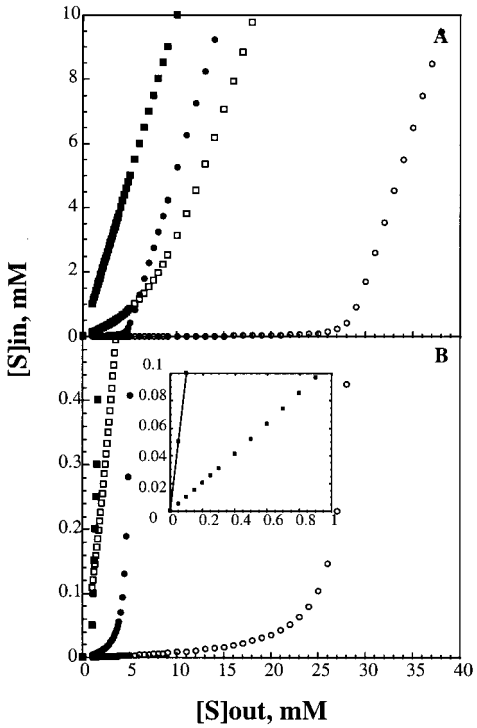

FIGURE 6: Levels of substrate in the periplasm. Panel A: Equation 2 was used to determine the concentration of substrate in the periplasm. The experimental values for PNPP were as follows: *E. coli* K12 pIV26 grown at 30 °C (●), $K_M = 1.5 \times 10^{-5}$ M and $[S_{out}]$ at $V_{max}/2 = 2.37 \times 10^{-3}$ M; *E. coli* O157:H7 pIV26 grown at 30 °C (○), $K_M = 1.5 \times 10^{-5}$ M and $[S_{out}]$ at $V_{max}/2 = 1.45 \times 10^{-2}$ M. The $[S_{in}]$ values for cephaloradine in *E. coli* K12 are shown (□), $K_M = 1.0$ mM, $[S_{out}]$ at $V_{max}/2 = 4.5$ mM (*29*). For comparison, $[S_{in}]$ vs $[S_{out}]$ is given for a bacterium without enzyme (■). Panel B: Expanded region of panel A. Panel B, insert: Expanded region of panel A for cephaloridine.

as reduced outer membrane permeability. For β-lactamase, enzyme expression levels may already approach an occupancy-limited state in the periplasm (*29*), and further improvements may depend on increase of enzyme efficiency (increase k_{cat} or decrease K_M) or on decrease of outer membrane permeability.

DISCUSSION

A unique feature of *E. coli* O157:H7 is an ability to survive divergent and hostile microenvironments so it can colonize and proliferate in the human intestinal tract (see ref *1*). For example, the osmolarity of well water is low relative to that of the human intestine. The pH of the stomach is low compared to that of water or intestine. Various antimicrobial agents such as bile salts are found in vivo. Tolerance to these situations may be enhanced by modified membrane permeability. This study focused on the outer membrane, which showed substantial deviation from wild-type *E. coli* with respect to its permeability and other properties. The implications of these changes were significant, including the description of bacterial properties which may contribute to virulance and the suggestion of possible future approaches to treatment and effective drug development.

The permeability of O157:H7 to an anionic compound, PNPP, was 2−6-fold lower than that of wild-type *E. coli*, depending on growth conditions. The larger difference occurred with growth at 30 °C, where wild-type *E. coli* expressed a high level of Omp F, the less restrictive porin. Growth at 37 °C resulted in lower permeability of wild-type *E. coli* due to increased expression of the more restrictive porin, Omp C. The O157:H7 strain did not show this physiological response to growth temperature, even though visual evaluation of protein staining in acrylamide gel electrophoretograms suggested that it expressed higher levels of Omp F when grown at lower temperature. While the detailed basis for a difference in permeability was not clear, it may arise from altered porin proteins.

The published sequence of the *E. coli* O157:H7 genome showed many altered proteins, including the porins of the outer membrane (*20*). The significance of these differences with respect to the pathogenicity of strain O157:H7 is not known. Omp C contains many changes, with only 93% identity to wild-type protein. Mass spectrometry verified all of these substitutions in the O157:H7 strain used in this study. While properties of Omp C of O157:H7 may be altered, wild-type Omp C is already a restrictive porin.

The Omp F of *E. coli* O157:H7 differs from wild-type protein by only two amino acids. Again, mass spectrometry verified these substitutions in the strain used in this study. The alterations were adjacent in the three-dimensional protein structure. While they did not alter the charge of the protein, they may alter the permeability by conformational change.

While altered permeability may arise from amino acid substitutions of porins in O157:H7, genomic sequence data alone could not explain the appearance of at least four bands which migrated in the region of porin proteins during gel electrophoresis. Mass spectrometry suggested that the four bands arose from the two porin proteins of O157:H7. Ion abundance in adjacent bands supported the presence of two forms of both Omp C and Omp F. No other proteins were identified in this region of the gel. The separation of the various porin bands was minimal, similar to that observed upon protein phosphorylation or other minor structural change. Thus, it was possible that a secondary modification of Omp C or Omp F proteins may occur and contribute to altered permeability. Candidates for change include post-translational modification such as hydrolysis of amine or peptide bonds or covalent modification by an unidentified structure. Another potential candidate for appearance of multiple bands is incomplete cleavage of the signal peptides of precursor proteins. Additional studies with HPLC−MS/MS have identified at least 75% of the expected peptides of each porin (data not shown). Further work will be needed to determine the basis for multiple bands of porin proteins in O157:H7.

If the basis for reduced permeability is a posttranslational protein modification rather than a genomic change, it is possible that inhibitors of the posttranslational enzyme(s) can be found. Such inhibitors may block modification, thereby converting O157:H7 to enhanced permeability and rendering it more susceptible to antimicrobial action. The permeability assay used in this study provided a facile method that might be used to screen for agents that change outer membrane permeability. The velocity of PNPP hydrolysis at low substrate is proportional to permeability, and a 6-fold difference between wild type and O157:H7 grown at 30 °C offers ready discrimination of wild type vs O157:H7 behavior.

Restriction of solute entry (acid and salts) into the periplasm could increase survival by reducing the challenge of maintaining periplasmic/cytoplasmic iso-osmolarity (*52*). In addition, a rigid inner and outer membrane would minimize the effects of an iso-osmolar shift. It may confer resistance against common antibacterial agents such as stomach acid, bile salts, and antibacterial peptides.

Lowered access to the periplasm can enhance antibiotic resistance. This is achieved by inactivation or pumping the antimicrobial agent out of the cell. Reduced entry through the outer membrane would enhance either of these actions. *E. coli* O157:H7 normally has resistance to sulfisoxazole, streptomycin, and tetracycline, all of which have cytoplasmic targets. A restrictive outer membrane should decrease the solute entry into the cell and increase the effectiveness of these antibiotic resistances.

Theoretical analysis of the behaviors of two enzymes, alkaline phosphatase and β-lactamase, showed the extent to which outer membrane permeability contributes to lowering the concentration of substrate in the periplasm and showed an enormous capacity to increase antibiotic resistance by evolution. Upon entering the periplasm, antibiotics such as the β-lactams become the substrates of two enzymes, the degradative β-lactamase that abolishes antibacterial action and the enzyme that is the target of the antibiotic. Survival will be greatest for a degradative enzyme with a low K_M (high affinity), by a high concentration of the degradative enzyme and by reduced access of the antibiotic to the periplasm. A common dose of ampicillin, 250 mg, should produce about 0.6 mM concentration in blood. This level is insufficient to saturate the β-lactamase enzymes in resistant *E. coli* (Figure 6). It is likely that antibiotic dose levels will remain on the horizontal portion of the Eadie−Hofstee plot shown in Figure 1, making bacteria resistant to standard treatment. Even if higher blood levels are used, theoretical simulations show an almost infinite ability of *E. coli* to increase resistance through evolution, including changes that create a more restrictive outer membrane (Figure 6).

An altered membrane was also suggested by transformation; *E. coli* O157:H7 was several thousand times less receptive than wild-type *E. coli*. Both the inner and outer membranes may contribute to this behavior. A qualitative observation which suggested an altered membrane was that *E. coli* O157:H7 required more passages through the French press to accomplish cell disruption. These properties suggest a more rigid membrane. Future studies may find that the modified porins contribute to this property as well.

Overall, this study showed several changes in membrane properties of O157:H7 that may contribute to enhanced survival. It appeared likely that permeability changes arose from porin proteins, either from amino acid changes in O157:H7 or from posttranslational modifications. While further investigations are needed to identify the actual basis for altered permeability and to determine its role in the high survival capabilities of O157:H7, the findings of this study offer a distinct phenotype that can be used for study and characterization. Future investigations may allow identification of compounds that assist in overcoming permeability barriers as a mechanism of antibiotic resistance without introduction of new antibiotics or use of antibiotics at high concentrations that are toxic to humans. In addition, the methods described in this study provide approaches to the study of other Gram-negative organisms that may have increased virulance due to a reduced outer membrane permeability.

REFERENCES

1. Kaper, J. B., and O'Brien, A. D. (1998) *Escherichia coli O157:H7 and other Shiga Toxin-Producing E. coli Strains*, ASM Press, Herndon, VA.
2. Bell, B. P., Goldoft, M., Griffin, P. M., Davis, M. A., Gordon, D. C., Tarr, P. I., Bartleson, C. A., Lewis, J. H., Barrett, T. J., Wells, J. G., et al. (1994) *J. Am. Med. Assoc. 272*, 1349−1353.
3. O'Brien, A. D., Newland, J. W., Miller, S. F., Holmes, R. K., Smith, H. W., and Formal, S. B. (1984) *Science 226*, 694−696.
4. O'Brien, A. D., Marques, L. R., Kerry, C. F., Newland, J. W., and Holmes, R. K. (1989) *Microb. Pathog. 6*, 381−390.
5. Jacewicz, M., Clausen, H., Nudelman, E., Donohue-Rolfe, A., and Keusch, G. T. (1986) *J. Exp. Med. 163*, 1391−404.
6. Karmali, M. A. (1989) *Clin. Microbiol. Rev. 2*, 15−38.
7. Keusch, G. T., Jacewicz, M., Acheson, D. W., Donohue-Rolfe, A., Kane, A. V., and McCluer, R. H. (1995) *Infect. Immun. 63*, 1138−1141.
8. Nakao, H., and Takeda, T. (2000) *J. Nat. Toxins 9*, 299−313.
9. Tilden, J., Jr., Young, W., McNamara, A. M., Custer, C., Boesel, B., Lambert-Fair, M. A., Majkowski, J., Vugia, D., Werner, S. B., Hollingsworth, J., and Morris, J. G., Jr. (1996) *Am. J. Public Health 86*, 1142−1145.
10. Karmali, M. A., Steele, B. T., Petric, M., and Lim, C. (1983) *Lancet 1*, 619−620.
11. Karmali, M. A., Petric, M., Lim, C., Fleming, P. C., Arbus, G. S., and Lior, H. (1985) *J. Infect. Dis. 151*, 775−782.
12. Louise, C. B., and Obrig, T. G. (1995) *J. Infect. Dis. 172*, 1397−1401.
13. Thayer, D. W., and Boyd, G. (1993) *Appl. Environ. Microbiol. 59*, 1030−1034.
14. Hayden, T. (1999) *Newsweek 134*, 37.
15. Spake, A. (1999) *U.S. News World Rep. 127*, 56.
16. Swerdlow, D. L., Woodruff, B. A., Brady, R. C., Griffin, P. M., Tippen, S., Donnell, H. D., Jr., Geldreich, E., Payne, B. J., Meyer, A., Jr., Wells, J. G., et al. (1992) *Ann. Intern. Med. 117*, 812−819.
17. Arnold, K. W., and Kaspar, C. W. (1995) *Appl. Environ. Microbiol. 61*, 2037−2039.
18. Horii, T., Barua, S., Kimura, T., Kasugai, S., Sato, K., Shibayama, K., Ichiyama, S., and Ohta, M. (1998) *Microbiol. Immunol. 42*, 871−874.
19. Waterman, S. R., and Small, P. L. (1996) *Infect. Immun. 64*, 2808−2811.
20. Perna, N. T., Plunkett, G., III, Burland, V., Mau, B., Glasner, J. D., Rose, D. J., Mayhew, G. F., Evans, P. S., Gregor, J., Kirkpatrick, H. A., Posfai, G., Hackett, J., Klink, S., Boutin, A., Shao, Y., Miller, L., Grotbeck, E. J., Davis, N. W., Lim, A., Dimalanta, E. T., Potamousis, K. D., Apodaca, J., Anantharaman, T. S., Lin, J., Yen, G., Schwartz, D. C., Welch, R. A., and Blattner, F. R. (2001) *Nature 409*, 529−533.
21. Nikaido, H., and Vaara, M. (1985) *Microbiol. Rev. 49*, 1−32.
22. Kim, H. H., Samadpour, M., Grimm, L., Clausen, C. R., Besser, T. E., Baylor, M., Kobayashi, J. M., Neill, M. A., Schoenknecht, F. D., and Tarr, P. I. (1994) *J. Infect. Dis. 170*, 1606−1609.
23. Kudva, I. T., Hatfield, P. G., and Hovde, C. J. (1996) *J. Clin. Microbiol. 34*, 431−433.
24. Marshall, N. J., and Piddock, L. J. (1997) *Microbiologia 13*, 285−300.
25. McMurry, L., Petrucci, R. E., Jr., and Levy, S. B. (1980) *Proc. Natl. Acad. Sci. U.S.A. 77*, 3974−3977.
26. Schnappinger, D., and Hillen, W. (1996) *Arch. Microbiol. 165*, 359−369.
27. Martinez, M. B., Schendel, F. J., Flickinger, M. C., and Nelsestuen, G. L. (1992) *Biochemistry 31*, 11500−11509.
28. Martinez, M. B., Flickinger, M. C., and Nelsestuen, G. L. (1996) *Biochemistry 35*, 1179−1186.

29. Martinez, M. B. (1995) in *Biochemistry, Molecular Biology and Biophysics*, p 156, University of Minnesota, St. Paul.
30. Schendel, F. J., Baude, E. J., and Flickinger, M. C. (1989) *Biotechnol. Bioeng. 34*, 1023−1036.
31. Glover, D. M. (1985) *DNA Cloning: A Practical Approach*, IRL Press, Oxford and Washington.
32. Ausubel, F. M., Brent, R., Kingston, R. E., Moore, D. D., Seidman, J. G., Smith, J. A., and Struhl, K. (2001) (Chanda, V. B., Ed.) *Current Protocols in Molecular Biology*, John Wiley & Sons, New York.
33. Adler, J. (1973) *J. Gen. Microbiol. 74*, 77−91.
34. Benson, S. A., and Decloux, A. (1985) *J. Bacteriol. 161*, 361−367.
35. Laemmli, U. K. (1970) *Nature 227*, 680−685.
36. Shevchenko, A., Wilm, M., Vorm, O., and Mann, M. (1996) *Anal. Chem. 68*, 850−858.
37. Guex, N., and Peitsch, M. C. (1997) *Electrophoresis 18*, 2714−2723.
38. Guex, N., Diemand, A., and Peitsch, M. C. (1999) *Trends Biochem. Sci. 24*, 364−367.
39. Peitsch, M. C. (1995) *Bio/Technology 13*, 658−660.
40. Martinez, M. B., Flickinger, M. C., and Nelsestuen, G. L. (1999) *J. Biotechnol. 71*, 59−66.
41. Nelsestuen, G. L., and Martinez, M. B. (1997) *Biochemistry 36*, 9081−9086.
42. Alphen, W. V., and Lugtenberg, B. (1977) *J. Bacteriol. 131*, 623−630.
43. Lugtenberg, B., Peters, R., Bernheimer, H., and Berendsen, W. (1976) *Mol. Gen. Genet 147*, 251−262.
44. Chai, T. J., and Foulds, J. (1977) *J. Bacteriol. 130*, 781−786.
45. Foulds, J., and Chai, T. (1979) *Can. J. Microbiol. 25*, 423−427.
46. Sugawara, E., and Nikaido, H. (1992) *J. Biol. Chem. 267*, 2507−2511.
47. Perkins, D. N., Pappin, D. J., Creasy, D. M., and Cottrell, J. S. (1999) *Electrophoresis 20*, 3551−3567.
48. Tatusova, T. A., and Madden, T. L. (1999) *FEMS Microbiol. Lett. 174*, 247−250.
49. Adachi, H., Ishiguro, M., Imajoh, S., Ohta, T., and Matsuzawa, H. (1992) *Biochemistry 31*, 430−437.
50. Moore, B. A., Jevons, S., and Brammer, K. W. (1979) *Antimicrob. Agents Chemother. 15*, 513−517.
51. Oka, T., Hashizume, K., and Fujita, H. (1980) *J. Antibiot. (Tokyo) 33*, 1357−1362.
52. Stock, J. B., Rauch, B., and Roseman, S. (1977) *J. Biol. Chem. 252*, 7850−7861.
53. Cowan, S. W., Schirmer, T., Rummel, G., Steiert, M., Ghosh, R., Pauptit, R. A., Jansonius, J. N., and Rosenbusch, J. P. (1992) *Nature* 358, 727−733.
54. Jeanteur, D., Schirmer, T., Fourel, D., Simonet, V., Rummel, G., Widmer, C., Rosenbusch, J. P., Pattus, F., and Pages, J. M. (1994) *Proc. Natl. Acad. Sci. U.S.A. 91*, 10675−10679.
55. Phale, P. S., Philippsen, A., Kiefhaber, T., Koebnik, R., Phale, V. P., Schirmer, T., and Rosenbusch, J. P. (1998) *Biochemistry 37*, 15663−15670.

BI0109515